THE JOURNAL OF PHYSICAL CHEMISTRY B

Article

pubs.acs.org/JPCB

Structural and Spectroscopic Properties of Water around Small Hydrophobic Solutes

Maria Montagna,[†] Fabio Sterpone,*[,‡] and Leonardo Guidoni*[,§]

[†]Dipartimento di Matematica Pura e Applicata, Università degli studi dell'Aquila, via Vetoio 1, 67010, L'Aquila, Italy

[‡]Laboratoire de Biochimie Théorique, CNRS, UPR9080, Université Paris Diderot, Sorbonne Paris Cité, 13 rue Pierre et Marie Curie, 75005, Paris, France

[§]Dipartimento di Scienze Fisiche e Chimiche, Università degli studi dell'Aquila, via Vetoio 1, 67010, L'Aquila, Italy

Supporting Information

ABSTRACT: We investigated the structural, dynamical and spectroscopic properties of water molecules around a solvated methane by means of Car−Parrinello molecular dynamics simulations. Despite their mobility, in the first shell, water molecules are dynamically displaced in a clathrate-like cage around the hydrophobic solute. No significant differences in water geometrical parameters, in molecular dipole moments or in hydrogen bonding properties, are observed between in-shell and out-shell molecules, indicating that liquid water can accommodate a small hydrophobic solute without altering its structural properties. The calculated contribution of the first-shell water molecules to the infrared spectra does not show significant differences with respect the bulk signal once the effects of the missing polarization of second-shell molecules has been taken into account. Small fingerprints of the clathrate-like structure appear in the vibrational density of states in the libration and OH stretching regions.

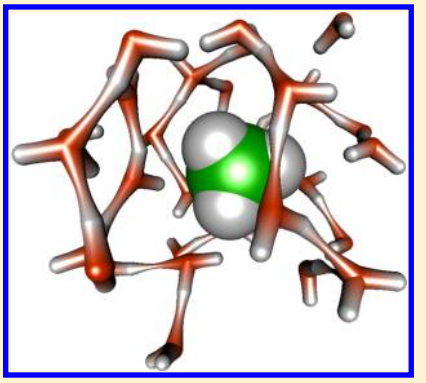

INTRODUCTION

Water structure and dynamics in proximity of hydrophobic solutes and surfaces are key for understanding processes involving hydrophobic interactions in very different contexts, e.g., molecular self-assembling, protein folding, ligand/protein docking, as well as nanoscale water confinement and surface wetting.

Vibrational (IR and Raman) spectroscopy is powerful to gain experimental insight on how a water hydrogen-bond (H-bond) network reorganizes close to hydrophobic solutes and interfaces. Water/organic liquid interfaces have been widely characterized using vibrational sum frequency spectroscopy (VSFS).[1,2] It was found that water has a weak intermolecular bonding character at the contact with the organic phase, and that a weak interaction with the organic molecules, mirrored by a red-shift of the dangling OH bond vibrations, forges the local orientation with effects on the mechanism of molecular absorption (e.g, polyelectrolytes) through the interface.[2,3] In a recent ab initio molecular dynamics (AIMD) study,[4] the weak interaction between water and a hydrophobic solid surface due to charge-fluctuations was seen to also affect the vibrational peak of the H-bonded OH of interfacial water. It was moreover appreciated by combining analytical modeling and classical simulation that a OH bond when pointing toward a hydrophobic surface-dangling state reorients faster than in neat water;[5] the quick rotation leads to a H-bonded state with a water partner.

A spectroscopic fingerprint of hydrophobic hydration is hard to extract for small particles or molecular groups in water solution since interfacial specificities risk being hidden by the bulk. The common picture supported by thermodynamics is that for small hydrophobic solutes, water forms a clathrate-like cage surrounding the apolar site here seen as a cavity in the water H-bonds network. For a simple methane molecule, NMR[6] and neutron diffraction[7] sized the hydration shell to about 17/20 water molecules.

A long-standing question concerns how the presence of the hydrophobic particle locally affects the strength and the exchange kinetics of the H-bonds forming the hydration cage, and ultimately how to experimentally make visible such a perturbation. Theoretical works have shown that water H-bonds are strengthened when water is confined between two small hydrophobic particles[8] or near hydrophobic groups in peptides.[9] Recently, the presence of dangling OHs was observed via vibrational Raman spectroscopy[10] also for water around the hydrophobic groups forming the alkyl tail of alcohols. This quite surprising result indicates that the clathrate-like picture for the hydration of atomistic-scale apolar groups should be softened by including a degree of structural disorder that in *rare events* produces observable free OH states for water. This finding agrees with the earlier simulative results,[11] describing how the local topology of hydrophobic patches in proteins influences the presence (or their relative fluctuations) of clathrate versus inverted orientations of water and how

Received: April 4, 2012
Revised: August 28, 2012
Published: September 4, 2012

frequently such disorder and fluctuations occur related to the perturbative effect of the hydrophobes on water reorientation, the underlying H-bond exchange reaction, and the connectivity dynamics. It was recently proposed, on the basis of time-resolved pump−probe infrared spectroscopy[12] and 2D-IR,[13] that the methyl groups of osmolytes (e.g., trimethylamine N-oxide (TMAO) and tetramethyl urea (TMU)) can freeze water inducing a great dynamical slow-down for the water OH reorientation. Theoretical investigations[14,15] and NMR experiments,[16] however, have seriously challenged this interpretation showing that the water slow-down is caused by the solute concentration rather than being an intrinsic feature of the hydrophobe/water interaction. In a dilute solution water retardation next to hydrophobes is mild due to a small excluded volume retardation factor.

As evident in the past literature, the interpretation of spectroscopic data largely benefits from complementary computational studies.[1,10,13−15,17] Here we present results from AIMD simulations of a methane/water solution with the aim to extract a spectroscopic fingerprint of hydrophobic hydration. We especially cared to understand how nuclear, electronic, and long-range correlations affect the IR spectrum of water surrounding the hydrophobic solute. In our simulations, van der Waals interactions, an essential key in modeling H-bonds,[18,19] were treated via the ad hoc potential, DCACP, developed by Röthlisberger et al.[20] Anticipating our main result, we see that water forms a rather dynamic cage around the hydrophobic particle with no significant perturbation of intra- and intermolecular interactions. We show that for water in the hydration shell around the methane, the electronic correlations with outer shell molecules affect the librational region of the spectrum similarly to what is observed in bulk water.

METHOD

System and Protocols. We used AIMD simulations to investigate the structural, dynamical, and vibrational properties of water molecules surrounding a molecule of methane. We considered a cubic box of size 12.5061 Å containing 63 water molecules and 1 methane.

The system was first equilibrated at ambient conditions using classical MD in the NVT ensemble (60 ps). A subsequent run in the NVE ensemble (60 ps) concluded the equilibration phase. These classical simulations were based on the Amber Force Field[21] for the methane and the TIP3P model for water.[22] Simulations were carried out using the Gromacs engine.[23]

The AIMD production run was carried out using the CPMD package[24] and the trajectory was evolved according to the Car−Parrinello integration scheme.[25] The electronic structure of the system was treated at the DFT level of theory with the BLYP functional[26] and the Kohn−Sham orbitals[27,28] expanded in plane waves with a cutoff of 70 Ry. Dispersive interactions were taken into account via dispersion corrected atom centered potentials (DCACP) developed by Röthlisberger and co-workers.[20] As reported in their works[20,29] DCACP models the long-range dispersive forces by an atom-electron interaction through the same analytical form as the nonlocal part of the Troullier−Martin pseudopotential.[30] In our simulations, the fictitious mass for the electronic degrees of freedom was set to 300 au and the time-step to 4 au. The simulation cell was a cubic box replicated in space with periodic boundary conditions. The cell volume was set to have the system at the experimental density of water. The system was first equilibrated at ambient temperature for 4 ps using the Nosé-Hoover thermostat.[31,32] The production run was carried out in the NVE ensemble for 70 ps. In order to check the statistical robustness of our analysis, we also produced four extra independent trajectories of different lengths 40−50 ps, starting from different initial configurations. An additional 20 ps simulation at higher temperature (actual average temperature 329 K) was carried out to monitor the dependence of our measured quantities on the changes of the water self-diffusion coefficient. In all cases, the trajectory was stored each simulation step, while the centers of maximally localizer Wannier functions[33] were stored each 10 simulation steps. For the sake of comparison, a pure water system of 64 molecules was simulated in the same thermodynamic conditions for 40 ps.

Analysis. The investigation of the vibrational properties of the system required the calculation of the water instantaneous molecular dipoles μ_i:

$$\mu_i = \mathbf{R}^i_{\mathrm{O}} + \mathbf{R}^i_{\mathrm{H}_1} + \mathbf{R}^i_{\mathrm{H}_2} - 2\sum_{c=1}^{4} \mathbf{R}^i_{\mathrm{w}_c} \tag{1}$$

where $\mathbf{R}^i_{\mathrm{O}}$, $\mathbf{R}^i_{\mathrm{H}_1}$, and $\mathbf{R}^i_{\mathrm{H}_2}$ are the nuclear coordinates of the ith molecule, and $\mathbf{R}^i_{\mathrm{w}_c}$ indicates the positions of the centers of the Wannier functions.

From the instantaneous values of μ_i, we computed the IR absorption coefficient per unit path length, by performing the Fourier Transform of the autocorrelation function of total dipole moment $\mathbf{M}(t) = \Sigma_i \mu_i(t)$:

$$\alpha(\omega) \propto \frac{2\pi\beta\omega^2}{3n(\omega)c}\int_{-\infty}^{+\infty} \mathrm{e}^{-i\omega t}\langle \sum_{ij} \mu_i(t)\cdot\mu_j(0)\rangle \,\mathrm{d}t \tag{2}$$

using a quantum correction factor obtained within the harmonic approximation, $n(\omega)$ being the refractive index of water, and $\beta = (1/k_{\mathrm{B}}T)$.[34]

The vibrational density of states (VDOS) was computed as the Fourier Transform of the autocorrelation function of the nuclear velocities

$$P(\omega) \propto \frac{2\pi\beta\omega^2}{3n(\omega)c}\int_{-\infty}^{+\infty} \mathrm{e}^{-i\omega t}\langle \sum_{ij} \mathbf{v}_i(t)\cdot\mathbf{v}_j(0)\rangle \,\mathrm{d}t \tag{3}$$

In order to investigate the local effect of the hydrophobic particle, we have restricted the averages in eq 2 and eq 3 to the water molecules belonging to the hydration shell of the methane, thus the time correlation function is extended only to those fragments of trajectory in which water molecules solvate the methane. The first hydration shell is defined using a spherical cutoff of 5 Å deduced by including the first peak of the radial distribution function $g_{\mathrm{COw}}(r)$ between the carbon atom of the methane and the oxygen atom of water (see Results section). The decomposition of $\alpha(\omega)$ in bulk and first shell components implies an approximation, since the cross-correlation between waters *in* and *out* the shell are neglected. The autocorrelation function of the total dipole, $\langle \mathbf{M}(0)\cdot\mathbf{M}(t)\rangle$, was decomposed in in-shell, out-shell, and cross-correlation terms:

$$\langle \mathbf{M}(0)\cdot\mathbf{M}(t)\rangle = \sum_{ij\subset \mathrm{Shell}} \langle \boldsymbol{\mu}_i(t)\cdot\boldsymbol{\mu}_j(0)\rangle + \sum_{ij\subset \mathrm{Bulk}} \langle \boldsymbol{\mu}_i(t)\cdot\boldsymbol{\mu}_j(0)\rangle + \sum_{i(j)\subset \mathrm{Shell};j(i)\subset \mathrm{Bulk}} \langle \boldsymbol{\mu}_i(t)\cdot\boldsymbol{\mu}_j(0)\rangle \tag{4}$$

The IR spectrum for the in-shell and out-shell water was obtained by considering separately the first and second terms of eq 4, respectively. We will carefully discuss the effect of the in/out shell cross-correlations on the IR spectra of water in the Results section. Spectra were smoothed *a posteriori* with Gaussians enveloping. The structure and dynamics of the methane hydration shell have also been investigated. We used the geometrical order parameter θ_t[35] to monitor the organization of the water H-bond network around the solute. The angle θ_t is the angle formed between the normal to the solute surface (here a sphere centered in the carbon atom) and each of the vectors that identify the four possible H-bonds of a water molecule. There are two possible orientations of water molecules around a hydrophobic solute: clathrate-like or inverted, or a mixture thereof. In clathrate-like orientation, three of the four vectors that describe the H-bonds in a water molecule are oriented tangential to the solute surface, and one points toward the bulk. The inverted orientation is specular to the previous one, characterizing maximal connectivity with outer-shell solvent.[36] The survival probability of water in the shell of the methane[37] as well as the reorientation of the water OH bond[14] for water initially in the shell have been computed for monitoring the shell/bulk exchange dynamics and the dynamic perturbation induced by the hydrophobe.

RESULTS

Structure and Dynamics of the Hydration Shell. In this first section, we monitor the structural properties of the methane hydration shell along with its dynamical character. The inclusion of DCACP in ab initio simulations of water recovers the correct description of the dispersion curve of the water dimer[18] as well as the dynamical properties of the liquid state.[20] At the same time, it improves the treatment of the water−methane interactions. To quantify the extent of such contribution, we calculated the difference of the binding energies between a methane and a water molecule with and without DCACP. Thanks to the improvement in the description of dispersive interactions, DCACP significantly increases the binding energy, which passes from Eb(BLYP) = −0.13 kcal/mol to Eb(DCACP) = −1.48 kcal/mol.

The radial distribution function of water oxygens with respect to the carbon atom ($g_{COw}(r)$) shows a peak at 3.8 Å and a first minimum at about 5 Å (Figure 1). On the basis of this structure, we defined the first hydration shell using a spherical cutoff of 5 Å. The resulting coordination number for the methane amounts to 17 water molecules (Figure 1), in agreement with experiments.[7,38] We point out that with respect to previous classical and ab initio MD simulations,[39] our model slightly enhances the first peak of the $g_{CO_w}(r)$ followed by a quite sharp decrease of the function toward the first minimum region.

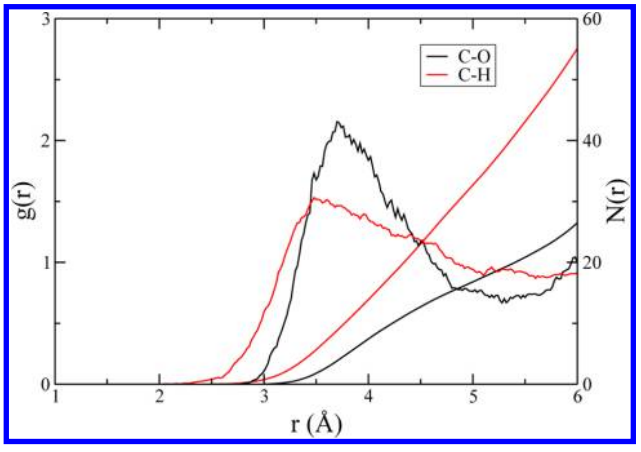

Figure 1. Radial distribution function $g(r)$ and coordination number $N(r)$ for C−O_w (black) and C−H_w pair-correlation functions.

It is well-known that water forms a clathrate-like structure around small hydrophobic particles with three of the four H-bond directions *caging* the apolar group. We recognize in our modeling such a structure. The distribution of $(1 - \cos \theta_t)$ plotted in Figure 2 is characterized by two peaks at the values θ_t = 0° and θ_t = 120°. This profile is typical of a clathrate-like configuration with three H-bonds forming an angle of about 120° with respect to the C−O_w axis (Figure 2). The cage formed around the methane does not distort the water−water connectivity, as proven by comparing several values of intra- and intermolecular parameters in waters, such as the OH bond lengths and HOH angles, the molecular dipole moment, and the number of H-bonds in the hydration shell and in the bulk. The average values for these parameters are reported in Table 1. Our finding shows that water can accommodate the apolar particle within its disordered H-bond network without major structural perturbation, in agreement with the results from neutron diffraction[7,40] and NMR[6] experiments and simulations.[41]

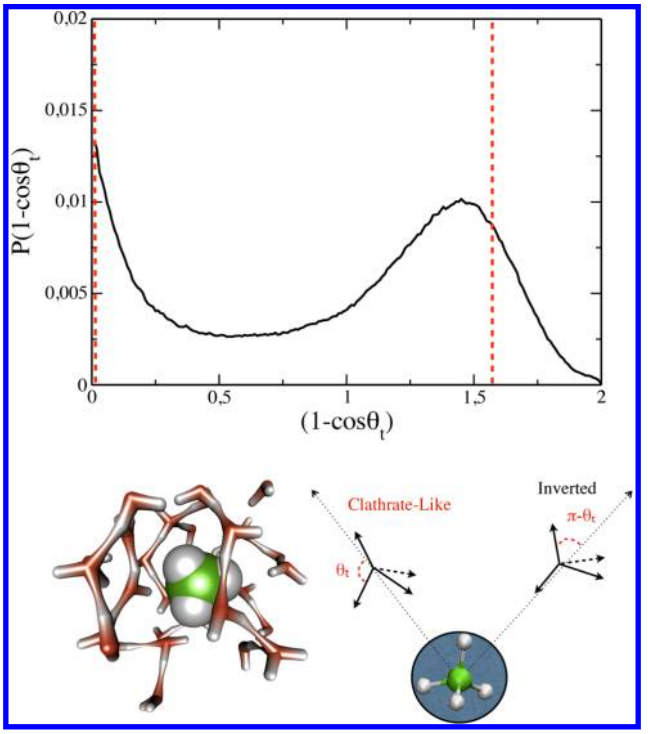

Figure 2. $(1 - \cos \theta_t)$ distribution for water molecules in the first hydration shell. The figure of methane in water was produced using the hyperballs plugin.[47]

It is now key to understand whether or not the water caging corresponds to a *frozen* state for the water−water network as proposed years ago by Frank and Evans[42] in their *iceberg* model of hydrophobic hydration. This model was recently invoked to interpret the results from pump−probe femtosecond infrared spectroscopy on concentrated osmolyte/water solutions.[12] It was actually proposed that the methyl groups of a osmolyte

dx.doi.org/10.1021/jp303213m | J. Phys. Chem. B 2012, 116, 11695−11700

Table 1. Structural and Electronic Properties[a]

	in-shell	out-shell	pure water
n-water	16.7 ± 1.7	46.2 ± 1.5	64
n-Hbond	3.2 ± 0.2	3.1 ± 0.1	2.8 ± 0.3
bond OH [Å]	1.0005(6)	1.0007(4)	1.0075(4)
angle (1-cos(θ°))	1.2661(7)	1.2654(4)	1.2651(3)
μ [D]	3.040(11)	3.039(4)	3.081(3)
$\mu_{\parallel}$ [D]	3.029(11)	3.026(4)	3.060(3)
$\mu_{\perp}$ [D]	−0.014(11)	−0.007(3)	0.010(3)

[a]Structural and electronic properties of water molecules in-shell and out-shell. We have decomposed water dipole moment into its components along the plane of the water molecule (xy) and along (z) the normal to this plane.

molecule (TMAO) induce a strong slowdown of water reorientation. However, the interpretation was severely challenged by theoretical[14] and experimental[16] works that showed the slow water dynamics to be caused by high solute concentration rather than by hydrophobic interaction.

To verify this interpretation, we computed the survival probability of water in the hydration shell and extracted the characteristic residence time for water by using a stretched-exponential fit. This characteristic time, τ_w, is about 4.7 ps, even if the exact value depends on how recrossing of the hydration shell is taken into account in the calculation (we have used a buffer time of t^* = 200 fs).[37] This is a clear signature of the dynamically labile nature of the methane hydration structure. A more precise signature comes from the calculation of the reorientation of the OH bond vectors of water initially residing in the methane hydration shell. [We computed the orientation time-correlation function (tcf) $\langle P_2[u(0)\cdot u(t)]\rangle$, where P_2 is the second-order Legendre polynomial, and $u(t)$ is the water OH bond vector at time t. The characteristic time is extracted by exponential fit in the time window of 2−6 ps. We find τ_2 = 5.5 ps for waters in-shell and τ_2 = 4.3 ps for waters in bulk.] The retardation factor with respect to bulk dynamics is ρ = 1.2. This finding is fully consistent with previous simulations[14,43] and experiments[16] showing that around a hydrophobic particle, the water−water H-bond exchange kinetics is only slightly retarded with respect to pure water. In fact, it was shown theoretically that this perturbation comes solely from an entropic excluded volume effect[14] that is rather weak for small hydrophobic particles in a dilute solution and that is seen to control water slowdown also in more complex biological systems as proteins.[44] Our results are in good agreement with a recent study of Rossato et al.[45] on hydrated methane, in which they predicted a moderate rotational slowing down of water molecules around the methane molecule. The water diffusion in the pure water and methane/water systems is slower than the experimental value at the same thermodynamic conditions, namely, the calculate diffusion coefficients are D = (0.080 ± 0.020) A^2/ps (at 308 K) and D = (0.076 ± 0.004) A^2/ps (at 309 K), respectively. However it should be noted that the calculated diffusivity in our systems is rather improved with respect to standard DFT/BLYP simulations that report for the same temperature a very low diffusion constant.[20,46] The better description of the water dynamical properties is ensured by the inclusion of the DCACP model. To investigate the role of the temperature on the dynamical properties with DCACP, we performed an additional 20 ps long simulation of the water/methane system at slightly higher temperature (326 K). We observed a higher value of the diffusion coefficient D = (0.20 ± 0.02) A^2/ps, whereas the vibrational properties and the spectral decomposition remained unchanged, as reported in the Supporting Information.

Vibrational Spectra. Let us now turn our attention to the spectroscopic properties of water in the hydration shell of the methane. According to the decomposition procedure described in the Method section (see eq 4), we have separated the IR spectra into in-shell and out-shell components. The spectrum resulting from these two terms, the total spectrum for water calculated for the water/methane system, and that obtained from the pure bulk water simulation are all compared in Figure 3. We appreciated that the line shapes of all three are very similar with a minor difference visible in the stretching region. In the water/methane solution, the peak shows a shoulder in the high frequency side of the peak, while for pure water the shoulder is present in the low frequency side. In the next step, we proceed to compare the individual in-shell and out-shell contributions reported in Figure 4.

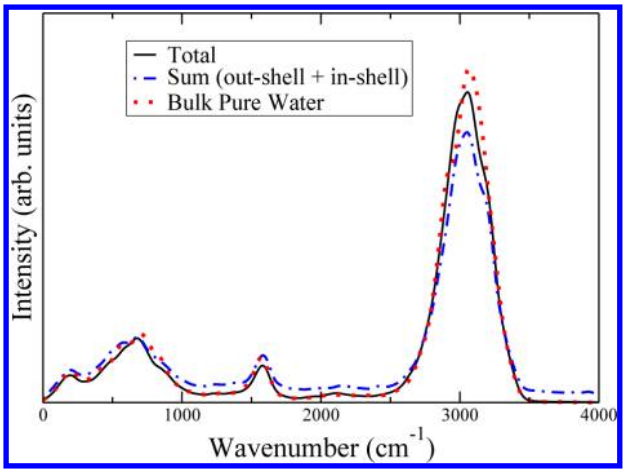

Figure 3. Comparison between *total* IR water spectrum and *sum* IR water spectrum obtained neglecting cross-correlations contribution between in-shell and out-shell water molecules.

First we note that the regions of the spectra associated with OH vibration and HOH bending are not strongly impacted by

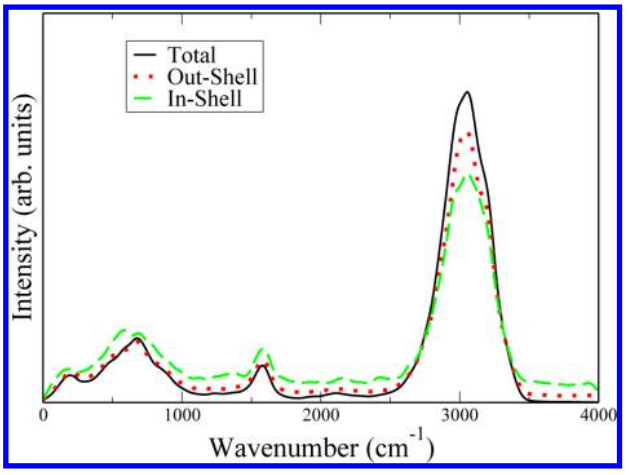

Figure 4. Decomposition of IR total water spectrum (black) into in-shell (green) and *out-shell* (red) contributions. The intensities are normalized with respect to the number of water molecules giving a contribution to the individual spectrum.

the presence of the solute. The intensity of the spectra clearly changes, but the position of the peaks is conserved. For the in-shell contribution, the peak is rather symmetric, while as observed before, the total and the out-shell contribution show a minor high frequency shoulder. The overall line shape confirms that the presence of a small hydrophobic particle has no influence on the strength of the H-bonds formed by the water molecules within its solvation shell. A rather different line shape is instead observed in the region associated to the molecular libration, (300−900) cm^{-1}. This difference is reproducible in all the blocks of length 10−20 ps, into which the whole trajectory can be fragmented. Hence we have investigated whether the somewhat enhanced structure visible around the frequency 600 cm^{-1} is a specific signature of the hydrophobic interaction or instead a consequence of the procedure employed to decompose the spectra. As a first step, we focused on the nuclear contribution to the spectra; this is achieved by decomposing the VDOS into in-shell and out-shell contributions. The spectra are reported in Figure 5, showing

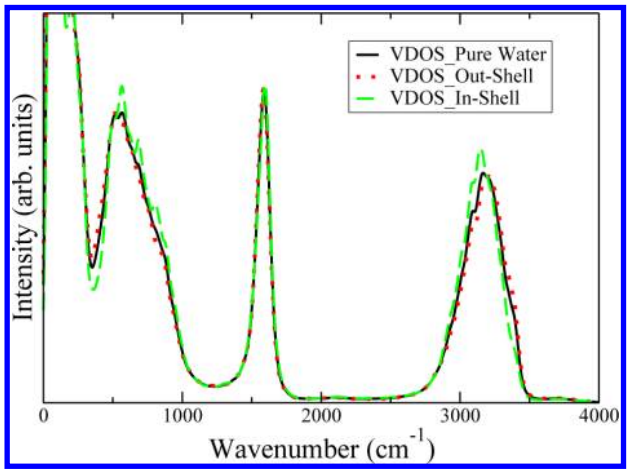

Figure 5. VDOS of pure water bulk (black). Decomposition of VDOS into in-shell (green) and out-shell (red) contributions.

unimportant differences between the densities of state associated with the solvation shell, the outer shell waters, and the whole system. The librational part of the in-shell water is somewhat more structured, and the vibrational region is slightly shifted with respect to the out-shell contribution and lacks the high-frequency shoulder.

These rather minor differences suggest that the structured IR spectrum line in the libration region should be traced back to electronic polarization effects. However, the direct calculation of properties depending on the electronic structure of the water molecules is not supportive of this hypothesis neither. The value of the dipole moment (and its components with respect to the water molecule plane) are equal for the in- and out-shells of water (see Table 1). Also, the time evolution of these values for the time spent in the hydration shell does not mark any specific behavior.

The lack of strong correlation between the nuclear, electronic properties of the hydration shell, and the IR line shape brought our attention to the in/out cross-correlation term neglected in decomposing the IR spectrum. In order to better understand the effect of these intermolecular correlations, we followed the strategy proposed by Marx and co-workers for investigating THz spectra of water.[17]

For this purpose we carried out an AIMD simulation of a small box of water (64 water molecules). The IR water spectrum was computed for water in the solvation shell of a tagged water molecule at increased value of the spherical cutoff radius defining the solvation shell. The results, reported in Figure 6, confirm within our ab initio model the finding

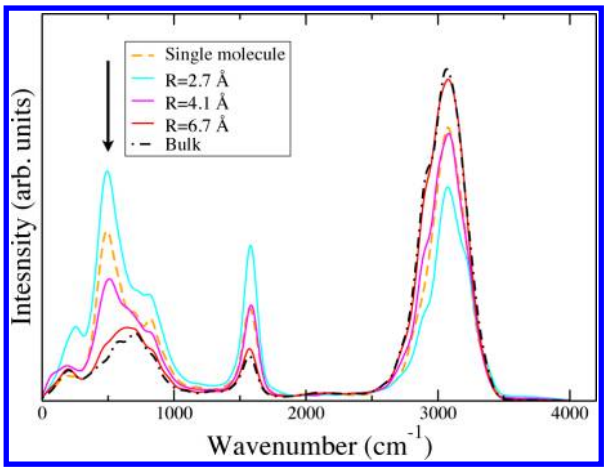

Figure 6. Decomposition of IR water spectrum as a function of an increasing cutoff radius. IR spectra for R = 0 (single molecule) (orange), R = 2.7 (cyan), R = 4.1 (magenta), R = 6.7 (red), and bulk limit (black).

previously reported by Marx and co-workers. By varying the cutoff radius, the line-shape of the IR libration region changes drastically, in particular, when the cutoff is increased, the structure around 600 cm^{-1} progressively disappears. A second neat effect is the shoulder flipping from the high to low frequency side of the stretching peak. This analysis supports the idea that the differences observed in the librational region of the IR spectrum associated to the hydration shell of the methane with respect to bulk are due to the neglected cross-correlation between in-shell and out-shell molecules. Unfortunately, the size of our system precludes a precise estimate of the spatial extension of these in/out correlations, but they should reasonably be of the same order of a pure water solution, about two shells. As already pointed out by Galli et al.,[4] the stretching peak is also affected by such cross-correlations; our analysis of the VDOS relates such effect to nuclear motion.

CONCLUSIONS

In this work we have investigated the structural, dynamical, and vibrational properties of water around a methane molecule via AIMD using a specifically designed potential for improving the description of dispersive interactions.[20] We found that water forms a dynamic clathrate-like cage around the hydrophobic particle. Water can accommodate this small solute without distorting its H-Bond network and preserving, on average, all its intramolecular parameters, such as OH bond length, HOH angle amplitude, and dipolar moment magnitude. A decomposition of the IR spectrum into in-shell and out-shell components indicates that the IR spectrum is not significantly altered by the presence of the methane, with the exception of the librational region of (300 − 900) cm^{-1}. We provide evidence that this difference is not a specific signature of hydrophobic hydration but rather an effect of the analysis itself, due to the removal of the dipole/dipole correlations between in-shell and out-shell water molecules. We suggest that,

dx.doi.org/10.1021/jp303213m | J. Phys. Chem. B 2012, 116, 11695−11700

similarly with what was observed for bulk water by Marx and co-workers,[17] in the hydration water of methane, the intensity of the librational part of the IR spectrum is sensitive to the presence of the second shell water molecules. Some small fingerprints of the clathrate-like structure appear in the VDOS in the region of the librations, which is slightly more structured, and in the region of the OH stretching. In the latter band, the VDOS signal of the first shell water molecules is missing a shoulder at high frequency, which is observed in both the out-shell and bulk cases.

■ ASSOCIATED CONTENT

Supporting Information

Dynamical properties and spectral decomposition of the same water/methane system at 326 K. This material is available free of charge via the Internet at http://pubs.acs.org.

■ AUTHOR INFORMATION

Corresponding Author

*E-mail: fabio.sterpone@ibpc.fr (F.S.); leonardo.guidoni@univaq.it (L.G.).

Notes

The authors declare no competing financial interest.

■ ACKNOWLEDGMENTS

The authors acknowledge computational resources provided by CASPUR computer center and CINECA computer center. We are grateful to M. Chavent and M. Baaden for having provided the plug-in Hyperballs used for graphical representation and to M. Barborini for reading the manuscript. F.S. acknowledges partial financial support from the European Research Council via the program IDEAS (Call ERC-2010-StG, ref. 258748-Thermos) and D.Laage for useful discussion. M.M. is grateful to V. Migliorati for the useful contribution in the structural analysis and to Eni spa for financial support within the Project "Un Ponte per L'Innovazione" (A Bridge for Innovation).

■ REFERENCES

(1) Scatena, L. F.; Richmond, G. L. *J. Phys. Chem. B* **2001**, *135*, 11240.
(2) Moore, F. G.; Richmond, G. L. *Acc. Chem. Res.* **2008**, *41*, 739−748.
(3) Beaman, D. K.; Robertson, E. J.; Richmond, G. L. *Proc. Natl. Acad. Sci. U.S.A.* **2012**, *109* (9), 3226−3231.
(4) Sharma, M.; Donadio, D.; Schwegler, E.; Galli, G. *Nano Lett.* **2008**, *8*, 2959−2962.
(5) Stirnemann, G.; Rossky, P. J.; Hynes, J. T.; Laage, D. *Faraday Discuss.* **2010**, *146*, 263−281.
(6) Dec, S. F.; Bowler, K. E.; Stadterman, L. L.; Koh, C. A.; Sloan, E. D. *J. Am. Chem. Soc.* **2006**, *128* (2), 414−415.
(7) Koh, C. A.; Wisbey, R. P.; Wu, X.; Westacott, R. E.; Soper, A. K. *J. Chem. Phys.* **2000**, *113*, 6390.
(8) Zichi, D. A.; Rossky, P. J. *J. Chem. Phys.* **1985**, *83*, 797.
(9) Matysiak, S.; Debenedetti, P. G.; Rossky, P. J. *J. Phys. Chem. B* **2011**, *115* (49), 14859−14865.
(10) Perera, P. N.; Fega, K. R.; Lawrence, C.; Sundstrom, E. J.; Tomlinson-Phillips, J.; Ben-Amotz, D. *J. Chem. Phys.* **2009**, *106* (30), 12230−12234.
(11) Cheng, Y. K.; Rossky, P. *Nature* **1998**, *392*, 696.
(12) Rezus, Y. L. A.; Bakker, H. J. *Phys. Rev. Lett.* **2007**, *99*, 148301(1)−(4).
(13) Bakulin, A. A.; Liang, C.; la Cour Jansen, T.; Wiersma, D. A.; Bakker, H. J.; Pshenichnikov, M. S. *Acc. Chem. Res.* **2009**, *42* (9), 1229.
(14) Laage, D.; Stirnemann, G.; Hynes, J. T. *J. Phys. Chem. B* **2009**, *113*, 2428−2435.
(15) Laage, D.; Stirnemann, G.; Sterpone, F.; Hynes, J. T. *Acc. Chem. Res.* **2012**, *45* (1), 53.
(16) Qvist, J.; Halle, B. *J. Am. Chem. Soc.* **2008**, *130*, 10345−10353.
(17) Heyden, M.; Sun, J.; Funkner, S.; Mathias, G.; Forbert, H.; Havenith, M.; Marx, D. *Proc. Natl. Acad. Sci. U.S.A.* **2010**, *107* (27), 12068.
(18) Sterpone, F.; Spanu, L.; Ferraro, L.; Sorella, S.; Guidoni, L. *J. Chem. Theory Comput.* **2008**, *4*, 1428.
(19) Jonchiere, R.; Seitsonen, A. P.; Ferlat, G.; Saitta, A. M.; Vuilleumier, R. *J. Chem. Phys.* **2011**, *135* (15), 154503.
(20) Lin, I. C.; Seitsonen, A. P.; Continho-Neto, M. D.; Tavernelli, I.; Rothlisberger, U. *J. Chem. Phys. B* **2009**, *113*, 1127−1131.
(21) Cornell, W. D.; Cieplak, P.; Bayly, C. L.; Gould, I. R.; Merz, K. M., Jr.; Ferguson, D. M.; Spellmeyer, D. C.; Fox, T.; Caldwell, J. W.; Koll-man., P. A. *J. Am. Chem. Soc.* **1995**, *117*, 5179.
(22) Jorgensen, W. L.; Chandrasekhar, J.; Madura, J. D.; Impey, R. W.; Klein, M. L. *J. Chem. Phys.* **1983**, *79*, 926.
(23) Hess, B.; Kutzner, C.; der Spoel, D. V.; Lindahl, E. *J. Chem. Theory Comput.* **2008**, *4*, 435.
(24) The code CPMD (http://www.cpmd.org) was used (2011).
(25) Car, R.; Parrinello, M. *Phys. Rev. Lett.* **1985**, *55*, 2471.
(26) Lee, C.; Yang, W.; Parr, R. *Phys. Rev. B.* **1988**, *37*, 785.
(27) Hohenberg, P.; Kohn, W. *Phys. Rev.* **1964**, *136*, B864.
(28) Kohn, W.; Sham, L. J. *Phys. Rev.* **1965**, *140*, A1133.
(29) von Lilienfeld, O. A.; Tavernelli, I.; Rothlisberger, U.; Sebastiani, D. *Phys. Rev. Lett.* **2004**, *93*, 153004.
(30) Troullier, N.; Martins, J. L. *Solid State Commun.* **1990**, *74*, 613.
(31) Nose, S. *Mol. Phys.* **1985**, *52*, 255.
(32) Hoover, W. *Phys. Rev. A* **1986**, *34*, 2499.
(33) Marzari, N.; Vanderbilt, D. *Phys. Rev. B* **1997**, *56*, 12847.
(34) Ramirez, R.; Ciudad, T. L.; Kumar, P. P.; Marx, D. *J. Chem. Phys.* **2004**, *121*, 3973.
(35) Cheng, Y.; Sheu, W. S.; Rossky, P. J. *Biophys. J.* **1999**, *76*, 1734−1743.
(36) Babiaczyk, W. I.; Bonella, S.; Guidoni, L.; Ciccotti, G. *J. Phys. Chem. B* **2004**, *114*, 15018.
(37) Impey, R. W.; Madden, P. A.; McDonald, I. R. *J. Phys. Chem.* **1983**, *87*, 5071.
(38) de Jong, P. H. K.; Wilson, J. E.; Neilson, G. W.; Buckingham, A. D. *Mol. Phys.* **1997**, *91*, 99.
(39) Grossman, J. C.; Schwegler, E.; Galli, G. *J. Phys. Chem. B* **2004**, *108*, 15865.
(40) Buchanan, P.; Soper, A. K.; Thompson, H.; Westacott, R. E.; Creek, J. L.; Hobson, G.; Koh, C. A. *J. Chem. Phys.* **2005**, *123*, 164507.
(41) Changman, M. P.; Taylor, P. C.; Rodger, P. M. *J. Am. Chem. Soc.* **2003**, *125*, 4706−4707.
(42) Frank, H. S.; Evans, M. W. *J. Chem. Phys.* **1945**, *13*, 507−532.
(43) Silvestrelli, P. L. *J. Phys. Chem. B* **2009**, *113*, 10728.
(44) Sterpone, F.; Stirnemann, G.; Laage, D. *J. Am. Chem. Soc.* **2012**, *134*, 4116−9.
(45) Rossato, L.; Rossetto, F.; Silvestrelli, P. L. *J. Phys. Chem. B* **2012**, *116*, 4552−4560.
(46) Kuo, I.-F. W.; Mundy, C. J.; McGrath., M. J.; Siepmann, J. I.; VandeVondele, J.; Sprik, M.; Hutter, J.; Klein, M. L.; Mohamed, F.; Krack, M.; Parrinello, M. *J. Phys. Chem. B* **2004**, *108*, 12990.
(47) Chavent, M.; Vanel, A.; Tek, A.; Levy, B.; Robert, S.; Raffin, B.; Baaden, M. *J. Comput. Chem.* **2011**, *32*, 2924.